Imaginary time Gaussian dynamics of the Ar_3 cluster

Holger Cartarius[1, a)] and Eli Pollak[1]
Chemical Physics Department, Weizmann Institute of Science, 76100 Rehovot, Israel

(Dated: 6 December 2010)

Semiclassical Gaussian approximations to the Boltzmann operator have become an important tool for the investigation of thermodynamic properties of clusters of atoms at low temperatures. Usually, numerically expensive thawed Gaussian variants are applied. In this article, we introduce a numerically much cheaper frozen Gaussian approximation to the imaginary time propagator with a width matrix especially suited for the dynamics of clusters. The quality of the results is comparable to that of thawed Gaussian methods based on the single-particle ansatz. We apply the method to the argon trimer and investigate the dissociation process of the cluster. The results clearly show a classical-like transition from a bounded moiety to three free particles at a temperature $T \approx 20\,\mathrm{K}$, whereas previous studies of the system were not able to resolve this transition. Quantum effects, i.e., differences with the purely classical case manifest themselves in the low-temperature behavior of the mean energy and specific heat as well as in a slight shift of the transition temperature. We also discuss the influence of an artificial confinement of the atoms usually introduced to converge numerical computations. The results show that restrictive confinements often implemented in studies of clusters can influence the thermodynamic properties drastically. This finding may have implications on other studies of atomic clusters.

PACS numbers: 36.40.-c, 03.65.Sq, 05.30.-d

I. INTRODUCTION

Rare gas atomic clusters are a topic of ongoing research partially due to the rich variety of their thermodynamic properties. Extensive studies have been carried out on structural transformations or phase transitions[1–7]. Properties of particular interest include the mean energy and specific heat. Computations on clusters of light atoms, e.g., Ne_{13} and Ne_{38}[1,2], predict novel low temperature quantum effects such as liquid-like zero temperature structures of Ne_{38} as compared to a solid-like structure predicted from classical mechanics[8].

The features in the mean energies or specific heats of such systems appear usually at low temperatures so that accurate quantum mechanical computational methods are essential. Accurate calculations for multidimensional systems, however, are challenging. Path-integral Monte Carlo methods[9–11] have been used to investigate rare gas clusters with up to a few dozen atoms, however, they become expensive for low temperatures so that approximations are necessary. Recently, new variants of semiclassical initial value representations have been adopted to problems involving the Boltzmann (imaginary time) operator $\exp(-\beta H)$. The time evolved Gaussian method developed by Mandelshtam and coworkers[3,12] has successfully been applied to atomic clusters[1–3,12,13] and dissipative systems[14]. It is based on the imaginary time propagation of a Gaussian wave packet of the form

$$\langle \boldsymbol{x}|g\rangle = \left(\pi^{3N}|\det \boldsymbol{G}(\tau)|\right)^{-1/4} \times \exp\left(-\frac{1}{2}[\boldsymbol{x}-\boldsymbol{q}(\tau)]^{\mathrm{T}}\boldsymbol{G}(\tau)^{-1}[\boldsymbol{x}-\boldsymbol{q}(\tau)]+\gamma(\tau)\right), \quad (1)$$

where for a cluster with N atoms the vectors are $3N$-dimensional and $\boldsymbol{G}(\tau)$ is a $3N \times 3N$-dimensional symmetric matrix of width parameters.

The time evolved Gaussian method can also become expensive for high dimensional systems. It belongs to the so-called *thawed* Gaussian methods, where the matrix of Gaussian width parameters $\boldsymbol{G}(\tau)$ changes with time. The number of the resulting equations of motion scales with N^2. This can become difficult when dealing with clusters of several dozen atoms. Thus, Mandelshtam and coworkers introduced the single-particle ansatz[3], in which the width matrix $\boldsymbol{G}(\tau)$ is reduced to a block-diagonal structure by only taking into account correlations of the coordinates of one particle and ignoring the inter-particle connections. With this approximation one has linear scaling ($6N$) with the number of atoms.

From a numerical point of view it is much cheaper to use *frozen* Gaussian representations of the thermal operator, in which the time-dependent width matrix $\boldsymbol{G}(\tau)$ in Eq. (1) is replaced by a constant matrix. The number of the remaining equations of motion which have to be solved scale as $3N$. Such a formalism has been provided by Zhang et al.[15]. One objective of this article is to apply the frozen Gaussian approach to the Boltzmann operator for a cluster of atoms. We will show that by an adequate nondiagonal choice of the constant width matrix, the frozen Gaussian method can accurately describe the mean energy, the specific heat, and signatures of dissociation processes. To do so, we will present a simple

a) Electronic mail: Holger.Cartarius@weizmann.ac.il

procedure to find a well suited shape for the width matrix. The results we obtain are of the same quality as the single-particle ansatz thawed Gaussian methodology, even though the frozen Gaussian variant leaves much less freedom to the Gaussian wave packet (constant width).

One cluster which has attracted the interest of theoretical investigations for a long time is the argon trimer[16–20], whose dissociation process has been discussed very recently in an extensive study[6]. In spite of its apparent simplicity with only three atoms involved, the thermodynamic properties at low temperatures $T < 40\,\mathrm{K}$ still include open questions. In particular, path-integral Monte Carlo calculations of the system[6] indicate a dissociation of the three atoms at temperatures $T \gtrapprox 35\,\mathrm{K}$ but cannot distinguish this process from structural changes. With the semiclassical Gaussian approximations discussed in this article we are able to provide well converged numerical mean energies and specific heats which exhibit an unambiguous classical-like dissociation at $T \approx 20\,\mathrm{K}$. We will also address the question of how important quantum effects are for the dissociation. Influences on the low temperature behavior of the mean energy and the specific heat will become observable and we will see that the transition temperature is shifted to a slightly lower value.

One focus of our discussion will be on the influence of an artificial confinement of the atoms. For converging numerical computations of the thermodynamic properties it is often necessary to restrict the configuration space to a certain volume by introducing an additional confining potential[7], which in practical applications usually is chosen to be very restrictive[1,3,4,7,13]. In this article we will show that such a restrictive choice can have a drastic influence on the dissociation process as was already discussed in a classical context many years ago[17]. This may have implications on other studies of atomic clusters.

The article is organized as follows. In Sec. II we introduce the Gaussian semiclassical approximation to the thermal operator. We review the thawed Gaussian (Sec. II A) propagator formalism and develop a new multidimensional form of its frozen Gaussian counterpart (Sec. II B) capable of competing with thawed Gaussian methods. The results for the argon trimer based on these semiclassical Gaussian methods are then presented in Sec. III. After introducing the system (Sec. III A) and comparing the Gaussian methods (Sec. III B) we discuss the influence of the confining potential on the thermodynamic properties (Sec. III C) and investigate the dissociation in the classical and the quantum case (III D). Conclusions are drawn in Sec. IV.

II. THERMAL OPERATOR FOR CLUSTERS AND GAUSSIAN APPROXIMATIONS

We consider a cluster of N atoms with only internal forces depending on the distance between the atoms, i.e., the Hamiltonian in mass scaled coordinates has the form

$$H = -\frac{\hbar^2}{2}\sum_{i=1}^{N}\Delta_i + \sum_{j<i} V(|\boldsymbol{r}_i - \boldsymbol{r}_j|), \tag{2}$$

where Δ_i is the Laplacian of particle i and $V(|\boldsymbol{r}_i - \boldsymbol{r}_j|)$ describes the two-body interaction between particles i and j, whose positions are given by the vectors $\boldsymbol{r}_i$. In the Gaussian representations used in this article it is necessary to evaluate integrals over a product of the potential with a coherent state, which are typically of the form

$$\langle h(\boldsymbol{q})\rangle = \int_{-\infty}^{\infty} d\boldsymbol{x}^{3N}\, \langle \boldsymbol{x}|g(\{y_i\})\rangle^2 h(\boldsymbol{x}), \tag{3}$$

where $\langle \boldsymbol{x}|g(\{y_i\})\rangle$ is a normalized coherent state in $\boldsymbol{x}$, which depends on a set of parameters $\{y_i\}$ usually including Gaussian positions $\boldsymbol{q}$ and a width matrix $\boldsymbol{G}$, e.g.,

$$\langle \boldsymbol{x}|g\left(\{y_i\} = \{\boldsymbol{q}, \boldsymbol{G}\}\right)\rangle = \left(\pi^{3N}|\det \boldsymbol{G}|\right)^{-1/4} \times \exp\left(-\frac{1}{2}[\boldsymbol{x}-\boldsymbol{q}]^{\mathrm{T}}\boldsymbol{G}^{-1}[\boldsymbol{x}-\boldsymbol{q}]\right). \tag{4}$$

The function $h(\boldsymbol{x})$ stands for the potential or one of its derivatives. The $3N$-dimensional vectors $\boldsymbol{x}$ and $\boldsymbol{q}$ combine the coordinates of all N atoms. It is essential for practical applications to reduce the numerical integrations as much as possible. Based on the facts that any central potential can be fitted by a sum of Gaussians and that a Gaussian in the distance $r_{ij} = |\boldsymbol{r}_i - \boldsymbol{r}_j|$ centered at the origin remains a Gaussian in Cartesian coordinates, Frantsuzov et al.[3] suggested the implementation of the interaction potential in terms of sums of Gaussians,

$$V(|\boldsymbol{r}_i - \boldsymbol{r}_j|) = \sum_p c_p e^{-\alpha_p r_{ij}^2}, \qquad r_{ij} = |\boldsymbol{r}_i - \boldsymbol{r}_j|, \tag{5}$$

so that all integrals of the form (3) can be evaluated analytically. This is of great advantage in numerical computations and is used for the work presented in this article.

To investigate the thermodynamic properties of the cluster we calculate the partition function $Z(\beta)$ by evaluating Gaussian initial value representations of the thermal operator

$$K(\beta) = e^{-\beta H}, \tag{6}$$

where $\beta = 1/(\mathrm{k}T)$ is the inverse temperature and $Z(\beta) = \mathrm{Tr}(K(\beta))$. We are interested in the mean energy $E = \mathrm{k}T^2\partial \ln Z/\partial T$ and the specific heat $C = \partial E/\partial T$. In our calculations we use two different semiclassical propagators based on a frozen and on a thawed Gaussian representation, where in both cases the Bloch equation

$$-\frac{\partial}{\partial \tau}|\boldsymbol{q}_0, \tau\rangle = H|\boldsymbol{q}_0, \tau\rangle \tag{7}$$

connected with the propagator (6) is approximately solved for a coherent state $|\boldsymbol{q}_0, \tau\rangle \approx |g(\{y_i\}, \tau)\rangle$ with either constant or variable Gaussian width parameters.

A. Thawed Gaussian representation

The thawed Gaussian representation of the thermal operator is the most versatile since it allows both the positions and widths of the Gaussian wave packet to vary with time. We consider the symmetrized time evolved Gaussian approximation (TEGA) suggested by Frantsuzov et al.[3,12],

$$\begin{aligned}\langle \boldsymbol{x}|K_{\mathrm{TG}}(\tau)|\boldsymbol{x}'\rangle = &\int \frac{d\boldsymbol{q}^{3N}}{(2\pi)^{3N}} \frac{\exp[2\gamma(\tau/2)]}{\det[\boldsymbol{G}(\tau/2)]} \\ &\times \exp\left(-\frac{1}{2}[\boldsymbol{x}-\boldsymbol{q}(\tau/2)]^{\mathrm{T}}\boldsymbol{G}(\tau/2)^{-1}[\boldsymbol{x}-\boldsymbol{q}(\tau/2)]\right) \\ &\times \exp\left(-\frac{1}{2}[\boldsymbol{x}'-\boldsymbol{q}(\tau/2)]^{\mathrm{T}}\boldsymbol{G}(\tau/2)^{-1}[\boldsymbol{x}'-\boldsymbol{q}(\tau/2)]\right),\end{aligned} \tag{8}$$

which is constructed from the coherent state

$$\begin{aligned}\langle \boldsymbol{x}|g(\{y_i\}=\{\boldsymbol{q}(\tau),\boldsymbol{G}(\tau)\})\rangle &= \langle \boldsymbol{x}|g(\boldsymbol{q}(\tau),\boldsymbol{G}(\tau))\rangle \\ &= \left(\pi^{3N}|\det \boldsymbol{G}(\tau)|\right)^{-1/4} \\ &\times \exp\left(-\frac{1}{2}[\boldsymbol{x}-\boldsymbol{q}(\tau)]^{\mathrm{T}}\boldsymbol{G}(\tau)^{-1}[\boldsymbol{x}-\boldsymbol{q}(\tau)]\right).\end{aligned} \tag{9}$$

One can then readily write down the partition function as:

$$Z_{\mathrm{TG}} = \int \frac{d\boldsymbol{q}^{3N}}{(2\sqrt{\pi})^{3N}} \frac{\exp[2\gamma(\tau/2)]}{\sqrt{\det[\boldsymbol{G}(\tau/2)]}}. \tag{10}$$

The width matrix $G(\tau)$ is symmetric positive definite. The Gaussian parameters follow the equations of motion in imaginary time τ,

$$\frac{d}{d\tau}\boldsymbol{G}(\tau) = -\boldsymbol{G}(\tau)\langle\nabla\nabla^{\mathrm{T}}V(\boldsymbol{q}(\tau))\rangle\boldsymbol{G}(\tau) + \hbar^2\mathbf{1}, \tag{11a}$$

$$\frac{d}{d\tau}\boldsymbol{q}(\tau) = -\boldsymbol{G}(\tau)\langle\nabla V(\boldsymbol{q}(\tau))\rangle, \tag{11b}$$

$$\frac{d}{d\tau}\gamma(\tau) = -\frac{1}{4}\mathrm{Tr}\left[\langle\nabla\nabla^{\mathrm{T}}V(\boldsymbol{q}(\tau))\rangle\boldsymbol{G}(\tau)\right] - \langle V(\boldsymbol{q}(\tau))\rangle, \tag{11c}$$

where $\langle\dots\rangle$ represents Gaussian averaged quantities of the form (3), which can be evaluated analytically for a potential (5) expressed in terms of Gaussians[3], and $\mathbf{1}$ is the $3N\times 3N$-dimensional identity matrix. The boundary conditions

$$\begin{aligned}&\boldsymbol{q}(\tau\approx 0) = \boldsymbol{q}_0, \qquad\qquad G(\tau\approx 0) = \hbar^2\mathbf{1}\tau, \\ &\gamma(\tau\approx 0) = -V(\boldsymbol{q}_0)\tau,\end{aligned} \tag{12}$$

are derived by demanding that in the limit $\tau\to 0$ the Gaussian approximation reduces to the identity operator.

In the framework of a Gaussian propagator the thawed Gaussian representation is usually the most accurate approximation to the exact quantum result due to the large freedom in the parameters, as has recently been demonstrated for a double well potential[21]. However, it is also the numerically most expensive method. The number of equations of motion for the width matrix (11a) scales with N^2, and the matrix operations at each time step even scale with N^3. This drastic increase in the required computing resources is the most critical drawback of the method. An attempt for combining the advantages of a thawed Gaussian propagator, where some matrix elements are still governed by the equations of motion (11a)-(11c), and avoiding the drawback of the expensive numerical effort to evaluate it, is achieved with the so-called "single-particle ansatz" of Frantsuzov et al.[3]. This ansatz, or variations of it, have been applied to several types of clusters[1,3,13]. It uses a block-diagonal matrix $\boldsymbol{G}(\tau)$, where 3×3 symmetric matrices representing one particle along the diagonal are the only non-vanishing matrix elements. Then the equations of motion (11a)-(11c) are only solved for the 3×3 blocks and only the corresponding 3×3 blocks of $\langle\nabla\nabla^{\mathrm{T}}V(\boldsymbol{q}(\tau))\rangle$ are included. In the single-particle ansatz the number of equations scales with N instead of N^2, however, one loses information in the non-diagonal 3×3 blocks, which are set to 0. Since the Gaussian propagators are in practical applications usually evaluated in Cartesian coordinates, in which the motions of the particles do not separate, important correlations between the particles are ignored. Thus, one expects that compared to the case of a full matrix the single-particle ansatz may lead to results of poorer quality.

In what follows we will call the full matrix variant of the thawed Gaussian propagator FC-TG (fully coupled thawed Gaussian, also referred to as the "fully coupled variational-Gaussian-wave-packet Monte Carlo" in Ref. 3) and the single-particle ansatz will be called SP-TG (single-particle thawed Gaussian, "single-particle variational-Gaussian-wave-packet Monte Carlo" in Ref. 3). For the argon trimer we will compare these respective approximations for the thermodynamic properties derived from the partition function with two variants of a frozen Gaussian propagator.

B. Frozen Gaussian representation

The frozen Gaussian representation of the thermal operator suggested by Zhang et al.[15] is based on a multidimensional frozen Gaussian coherent state

$$\begin{aligned}\langle \boldsymbol{x}|g(\{y_i\}=\{\boldsymbol{p}(\tau),\boldsymbol{q}(\tau),\boldsymbol{\Gamma}\})\rangle &= \langle \boldsymbol{x}|g(\boldsymbol{p}(\tau),\boldsymbol{q}(\tau),\boldsymbol{\Gamma})\rangle \\ &= \left(\frac{\det(\boldsymbol{\Gamma})}{\pi^{3N}}\right)^{1/4} \exp\Big(-\frac{1}{2}[\boldsymbol{x}-\boldsymbol{q}(\tau)]^{\mathrm{T}}\boldsymbol{\Gamma}[\boldsymbol{x}-\boldsymbol{q}(\tau)] \\ &\qquad + \frac{i}{\hbar}\boldsymbol{p}^{\mathrm{T}}(\tau)\cdot[\boldsymbol{x}-\boldsymbol{q}(\tau)]\Big),\end{aligned} \tag{13}$$

where $\boldsymbol{\Gamma}$ is in general a $3N\times 3N$-dimensional constant width matrix with positive eigenvalues, and $\boldsymbol{q}(\tau)$ and $\boldsymbol{p}(\tau)$ describe the dynamical variables. The symmetrized

frozen Gaussian approximation to the propagator reads

$$\begin{aligned}\langle \boldsymbol{x}'|K_{\mathrm{FG}}(\tau)|\boldsymbol{x}\rangle &= \det(\boldsymbol{\Gamma})\exp\left(-\frac{\hbar^2}{4}\mathrm{Tr}(\boldsymbol{\Gamma})\tau\right)\\ &\times\sqrt{\det\left(2\left[\mathbf{1}-\exp(-\hbar^2\boldsymbol{\Gamma}\tau)\right]^{-1}\right)}\\ &\times\exp\left(-\frac{1}{4}[\boldsymbol{x}'-\boldsymbol{x}]^{\mathrm{T}}\boldsymbol{\Gamma}[\tanh(\hbar^2\boldsymbol{\Gamma}\tau/2)]^{-1}[\boldsymbol{x}'-\boldsymbol{x}]\right)\\ &\times\int_{-\infty}^{\infty}\frac{d\boldsymbol{q}^{3N}}{(2\pi)^{3N}}\exp\Bigg(-2\int_0^{\tau/2}d\tau\langle V(\boldsymbol{q}(\tau))\rangle\\ &\quad-[\bar{\boldsymbol{x}}-\boldsymbol{q}(\tau/2)]^{\mathrm{T}}\boldsymbol{\Gamma}[\bar{\boldsymbol{x}}-\boldsymbol{q}(\tau/2)]\Bigg)\end{aligned}\tag{14}$$

with $\bar{\boldsymbol{x}}=(\boldsymbol{x}'+\boldsymbol{x})/2$ and the Gaussian averaged potential $\langle V(\boldsymbol{q}(\tau))\rangle$ is as defined in Eq. (3). Taking the trace yields the partition function[15]

$$\begin{aligned}Z_{\mathrm{FG}}(\tau)=\mathrm{Tr}\left[K_{\mathrm{FG}}(\tau)\right] &= \sqrt{\det(\boldsymbol{\Gamma})}\exp\left(-\frac{\hbar^2}{4}\mathrm{Tr}(\boldsymbol{\Gamma})\tau\right)\\ &\times\sqrt{\det\left(\left[\mathbf{1}-\exp(-\hbar^2\boldsymbol{\Gamma}\tau)\right]^{-1}\right)}\\ &\times\int_{-\infty}^{\infty}\frac{d\boldsymbol{q}^{3N}}{(2\pi)^{N/2}}\exp\left(-2\int_0^{\tau/2}d\tau\langle V(\boldsymbol{q}(\tau))\rangle\right).\end{aligned}\tag{15}$$

The numerical evaluation is relatively simple since one only needs to solve the $3N$ imaginary time equations of motion

$$\frac{\partial\boldsymbol{q}(\tau)}{\partial\tau}=-\boldsymbol{\Gamma}^{-1}\langle\nabla V(\boldsymbol{q}(\tau))\rangle\tag{16}$$

for the Gaussian positions $\boldsymbol{q}(\tau)$ and only one configuration space integration over the initial positions $\boldsymbol{q}(\tau=0)$ has to be performed.

As in the case of the SP-TG propagator the numerical scaling in the evaluation of the two-body potential terms is N^2. The numerical advantage of the frozen Gaussian propagator as compared to the FC-TG or SP-TG methods is due to the constant width matrix, i.e., one has only to propagate the equations of motion (16), whose number scales with N. Additionally, functions of the width matrix $\boldsymbol{\Gamma}$ can be evaluated in advance and do not have to be repeated at every time step since $\boldsymbol{\Gamma}$ does not evolve in time. On the other hand, the width matrix $\boldsymbol{\Gamma}$ is a parameter of the system and its actual choice has a critical impact on the quality of the results[15]. It is not trivial to find a good choice of $\boldsymbol{\Gamma}$, however, the problem simplifies when all particles are identical.

For N identical particles the simplest structure for $\boldsymbol{\Gamma}$ is a diagonal matrix with identical width elements, i.e., a multiple of the $3N\times 3N$ identity matrix,

$$\boldsymbol{\Gamma}_1=\Gamma\mathbf{1},\tag{17}$$

with only one parameter Γ. This ansatz treats all particles equally, is very simple to implement, and has the lowest numerical cost due to the diagonal structure of the matrix in Cartesian coordinates. However, it ignores the fact that a correct description of the cluster has to contain both the free motion of the center of mass and the relative motion determined by the particle-particle interaction potential (5).

In a frozen Gaussian approximation the exact partition function of a free particle is obtained in the limit of a vanishing Gaussian width [cf., e.g., Eq. (15)], whereas the optimum width for the relative coordinates can be deduced from a harmonic approximation around the minimum of the particle-particle interaction potential and has a finite value. A separation of the free motion of the center of mass from the internal degrees of freedom should be avoided since it complicates the structure of the equations of motion by introducing numerically more expensive terms such as a non-diagonal mass matrix. Considering the thawed Gaussian propagators we note that the FC-TG is capable of correctly describing the free center of mass motion when it is combined with an internal potential independently of the choice of the coordinate system, whereas this is not fulfilled for the SP-TG[3,22].

In the following we suggest a procedure based on an adequate choice of the width matrix which allows for a correct description of the free center of mass motion without changing the structure of the equations. To simplify, we restrict our description to the case of three particles relevant to this article, a generalization to an arbitrary number of particles is straightforward. It is plausible that in a system of coordinates $\boldsymbol{R}_i$ for the center of mass

$$\boldsymbol{R}_{\mathrm{cm}}=\frac{1}{3}\left(\boldsymbol{r}_1+\boldsymbol{r}_2+\boldsymbol{r}_3\right)\tag{18a}$$

and the two relative positions

$$\boldsymbol{R}_1=\boldsymbol{r}_1-\boldsymbol{r}_2,\tag{18b}$$

$$\boldsymbol{R}_2=\boldsymbol{r}_1-\boldsymbol{r}_3\tag{18c}$$

a diagonal matrix structure is a good choice. In these coordinates the center of mass is separated and we introduce the Gaussian width parameter D_1 for its motion. The Gaussian approximation becomes exact for the center of mass motion in the limit $D_1\to 0$. Since all particles are equal and there is no motivation for distinguishing between the propagation of the individual relative coordinates, we use one single parameter D_2 for the remaining coordinates. The matrix which then is applied to the coordinates (18a)-(18c) is

$$\boldsymbol{\Gamma}_{\mathrm{cmc}}=\begin{pmatrix}\boldsymbol{D}_1 & \mathbf{0} & \mathbf{0}\\ \mathbf{0} & \boldsymbol{D}_2 & \mathbf{0}\\ \mathbf{0} & \mathbf{0} & \boldsymbol{D}_2\end{pmatrix},\tag{19}$$

where $\boldsymbol{D}_1$ and $\boldsymbol{D}_2$ are 3×3 diagonal matrices with coefficients D_1 and D_2, respectively, and $\mathbf{0}$ is a 3×3 matrix of zeros. The most efficient way to evaluate the frozen Gaussian partition function is to keep its structure (15)

TABLE I. Parameters used in the Gaussian fit (5) of the Morse potential (21).

p	c_p [cm^{-1}]	α_p [Å^{-2}]
1	3.296×10^5	0.6551
2	-1.279×10^3	0.1616
3	-9.946×10^3	6.0600

in Cartesian coordinates and to transform the width matrix into the Cartesian system $\boldsymbol{r}_1$, $\boldsymbol{r}_2$, $\boldsymbol{r}_3$, i.e.,

$$\boldsymbol{\Gamma} = \begin{pmatrix} (\boldsymbol{D}_1+2\boldsymbol{D}_2)/3 & (\boldsymbol{D}_1-\boldsymbol{D}_2)/3 & (\boldsymbol{D}_1-\boldsymbol{D}_2)/3 \\ (\boldsymbol{D}_1-\boldsymbol{D}_2)/3 & (\boldsymbol{D}_1+2\boldsymbol{D}_2)/3 & (\boldsymbol{D}_1-\boldsymbol{D}_2)/3 \\ (\boldsymbol{D}_1-\boldsymbol{D}_2)/3 & (\boldsymbol{D}_1-\boldsymbol{D}_2)/3 & (\boldsymbol{D}_1+2\boldsymbol{D}_2)/3 \end{pmatrix}. \tag{20}$$

This procedure requires the implementation of a full width matrix in the numerical evaluation of the frozen Gaussian thermal operator but avoids a full mass matrix and a change in the structure of the propagator. The results for the argon trimer presented in Sec. III B will show that despite its simplicity this choice leads to results which are competitive with the SP-TG propagator even though this variant of the frozen Gaussian propagator is much cheaper to evaluate numerically.

To distinguish the frozen Gaussian propagator with the matrix structure of Eq. (20) from its diagonal variant we will refer in the following to the two approximations as 2P-FG (two-parameter frozen Gaussian) and 1PD-FG (one-parameter diagonal frozen Gaussian), respectively.

III. THE ARGON TRIMER

A. Atomic parameters and numerical procedure

To be able to compare our results with previous investigations of the argon trimer[6,16] we express the pairwise interaction by means of a Morse potential

$$V(r_{ij}) = D\left(\exp\left[-2\alpha(r_{ij}-R_\mathrm{e})\right] - 2\exp\left[-\alpha(r_{ij}-R_\mathrm{e})\right]\right) \tag{21}$$

where r_{ij} is the distance between particles i and j. The Morse parameters are listed in Ref. 16 and have been chosen such that the Morse potential reflects a previous fit to experimental results[23]. They are $D = 99.00\,\mathrm{cm}^{-1}$, $\alpha = 1.717\,\text{Å}$, and $R_\mathrm{e} = 3.757\,\text{Å}$. Using the three sets of Gaussian parameters listed in Table I we achieved a very accurate Gaussian fit to this Morse potential with a standard deviation smaller than $0.4\,\mathrm{cm}^{-1}$ in the relevant region between $r = 3.2\,\text{Å}$ and $r = 6\,\text{Å}$ around the minimum. As will become clear below this deviation is much smaller than effects due to the Gaussian approximation used to calculate the quantum mean energy, i.e., differences with the previous studies of the system[6,16] do not originate from the Gaussian fit of the potential, which is only introduced to accelerate numerical computations.

In numerical evaluations of the partition function it is essential to restrict the position space integrations [cf. $\boldsymbol{q}$ integrations in Eqs. (10) and (15)] to a reasonable region of the configuration space containing all relevant information about the thermodynamics of the cluster. Usually, this is done by introducing an additional steep potential located at a certain distance R_c from the center of mass $\boldsymbol{R}_\mathrm{cm}$, e.g.,

$$V_\mathrm{c}(\boldsymbol{r}) \propto \sum_{i=1}^{N} \left(\frac{\boldsymbol{r}_i - \boldsymbol{R}_\mathrm{cm}}{R_\mathrm{c}}\right)^{20} \tag{22}$$

(cf. Ref. 4) or, as implemented in our numerics, by restricting the sampling points $\boldsymbol{q}(\tau=0)$ in the integrations to values $|\boldsymbol{q}-\boldsymbol{R}_\mathrm{cm}| < R_\mathrm{c}$. If the radius of the confining sphere is chosen correctly, the restriction or its explicit form should have no influence on the results. The Monte Carlo sampling in $\boldsymbol{q}$ is done with a standard Metropolis algorithm, where we followed the procedure suggested by Frantsuzov et al. explained in detail in Ref. 3.

The optimum width parameter connected with the atom-atom interaction in the two parameter ansatz (20) of the frozen Gaussian propagator was found to be $D_2 = 25\,\text{Å}^{-2}$ by using several choices, monitoring the results, and comparing them to the thawed Gaussian methods. For this choice of the parameter D_2 the low-temperature mean energy reaches the smallest value, i.e., a minimum when plotted vs. D_2, thus, representing the best approximation to the ground level. The observation of the smallest energy value in the limit $T \to 0$ can be used as an additional criterion independently of the availability of a second method such as the thawed Gaussian propagator. We note that one can also monitor the relative amplitude of higher order corrections to the Gaussian approximation[15,21,24] as a function of the width parameters.

A value of $D_1 = 0.1\,\text{Å}^{-2}$ is already small enough to lead to the best possible description of the free center of mass motion. Using even smaller values for D_1 did not change the results, so we decided to use this value to have a well conditioned matrix of which the eigenvalues do not differ too much in their order of magnitude. The parameter for a diagonal matrix in the 1PD-FG propagator representing the best middle ground between D_1 and D_2 is $\Gamma = 20\,\text{Å}^{-2}$. It was selected with the method described for D_2 above. In a previous study of the frozen Gaussian imaginary time propagator it was found that the optimum choice for the width parameter is almost independent of the temperature[15], this was also confirmed in our study of the argon trimer. We found that the radius of the confining sphere does not have a significant influence on the optimum choice for the width matrices. Indeed, by checking several values as described above, it turned out that working with the same values for all computations was the best choice.

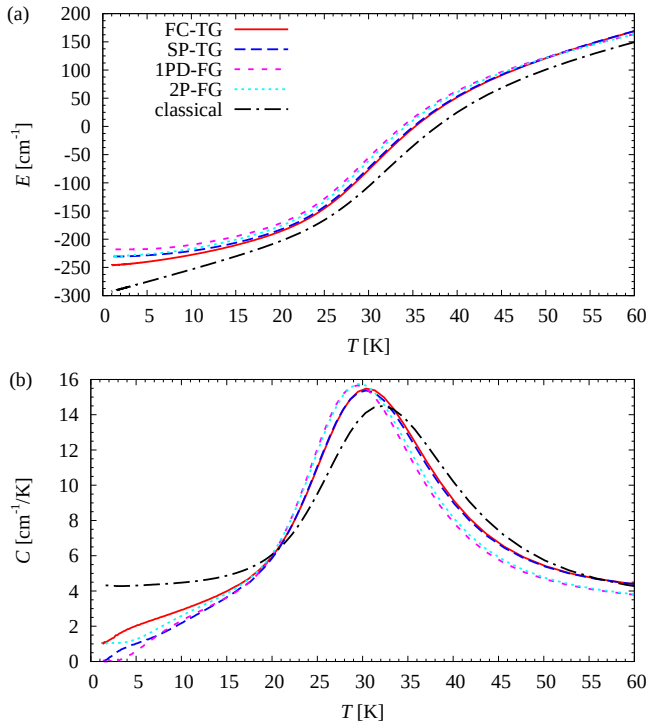

FIG. 1. Mean energy (a) and specific heat (b) of the argon trimer calculated for a confining radius of $R_c = 10$ Å. Results are provided for the thawed Gaussian approximations FC-TG and SP-TG, the frozen Gaussian approximations 1PD-FG, 2P-FG, and the classical theory.

B. Comparison of the Gaussian imaginary time propagators

First we investigated the different methods introduced in Sec. II for the evaluation of the quantum partition function for the argon trimer. To compare our results with the previous path-integral Monte-Carlo calculation by Pérez de Tudela et al.[6] we selected one of their parameter sets and calculated the mean energy and the specific heat for the argon trimer enclosed by a confining sphere with a radius of 10 Å, which is the weakest confinement applied in their study. Our results obtained with the four Gaussian propagators described above are also compared with the corresponding derivatives of the classical partition function

$$Z_{\mathrm{cl}} = \left(\frac{\mathrm{k}T}{2\pi\hbar^2}\right)^{3/2N} \int e^{-\beta V(\boldsymbol{q})}\, d\boldsymbol{q}^{3N}. \qquad (23)$$

They are presented in Fig. 1. To allow for the comparison with the path-integral Monte Carlo computations of Ref. 6 in Fig. 2 we subtracted for this figure the exact kinetic energy of the free center of mass $E_{\mathrm{cm}} = 3/2\mathrm{k}T$ from our values, which, in the calculation, always include the energy of the whole cluster including the center of mass translation.

The four semiclassical methods are in reasonably good agreement with each other and the classical results, however, there are quantitative differences. One can expect that the thawed Gaussian imaginary time propagator with a full matrix (FC-TG) provides the best approximation to the exact quantum results, and indeed the mean energy obtained with that method shows the best correspondence with the path-integral Monte Carlo computations of Ref. 6 (cf. Fig. 2). In particular, in the low-temperature limit the FC-TG propagator gives the best approximation ($E = -246\,\mathrm{cm}^{-1}$) to the ground state energy[6] of $-252.44\,\mathrm{cm}^{-1}$. Even though the FC-TG method is the most versatile propagator applied here, it still assumes a Gaussian form of the atom's wave functions and shows a slight difference as compared to the numerically exact path-integral Monte Carlo ground state energy. For higher temperatures there appear larger deviations as compared to the path-integral Monte Carlo results of Ref. 6, however, the latter ones are not very accurate due to the larger statistical error with increasing temperature. The semiclassical Gaussian approximations are expected to describe the partition function and its derivatives at higher temperatures even better than at low temperatures since they converge to the correct answer in the classical limit. We can thus assume that our results are more accurate as the temperature increases. The differences between our results and those of Ref. 6 at higher temperatures $T \gtrapprox 30$ K become even clearer when considering the specific heat. Our Gaussian calculations indicate a direct transition from the bound cluster to the completely dissociated situation with three free atoms, whereas such a clear conclusion is not possible with the path-integral Monte Carlo calculations of Ref. 6. This transition is discussed in more detail in the next two sections.

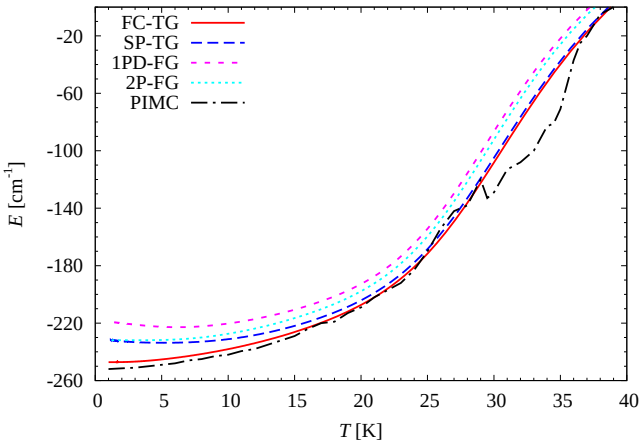

FIG. 2. Comparison of the mean energy obtained with the Gaussian methods FC-TG, SP-TG, 1PD-FG, and 2P-FG with the path-integral Monte-Carlo (PIMC) values taken from Ref. 6. The kinetic energy of the free center of mass motion is subtracted from our results to allow for the comparison.

It is also expected that the worst approximation in the low-temperature limit is obtained by the 1PD-FG ansatz.

As was mentioned in Sec. II B the diagonal width matrix does not treat the free center of mass motion correctly. This manifests itself as a large deviation of the mean energy from the correct value for $T \to 0$. The energy calculated with the diagonal frozen Gaussian width matrix increases for temperatures below 5 K, and this is definitely wrong. This deficiency is overcome with the 2P-FG matrix as presented in Eq. (20). It leads to a considerably lower mean energy in the low-temperature limit, which is closer to the exact ground level and is also closer to the FC-TG energy values, which can be considered to provide the best values of all methods used here.

More interesting, however, is the comparison of the 2P-FG and the SP-TG propagators. As reported in previous investigation of larger clusters[3] the single-particle thawed Gaussian approximation shows results for the mean energy and the specific heat which are qualitatively in agreement with the full matrix case. Quantitative differences have been reported and can also be found in our calculations for temperatures $T \lessapprox 45$ K. The differences with respect to the full matrix results increase with decreasing temperature. However, as can be seen in Fig. 1(a) the description of the mean energy of the SP-TG and the 2P-FG methods is of similar quality at very low temperatures. This is a remarkable finding since the evaluation of the single-particle thawed Gaussian propagator is more expensive than the frozen Gaussian due to the need to propagate the width matrix elements in time.

By contrast, the specific heat curve of the 2P-FG propagator is closer to that of the 1PD-FG than to the two thawed Gaussian approximations which agree very well with each other. It seems that in the temperature region around the transition from the bound to the dissociated cluster, a thawed Gaussian can provide a better description. However, the deviation is small and vanishes for weaker external confinements. An example for such a weaker confinement is shown in Fig. 3, in which the comparison of Fig. 1 is repeated for a confinement of $R_c = 32$ Å. Here, down to a temperature of 18 K the two thawed Gaussian approximations and the 2P-FG propagator provide almost identical results. The lines lie on top of each other both for the mean energy and the specific heat. Only the 1PD-FG values deviate a bit from the three other methods.

In summary, we can state that the thawed Gaussian propagator with a full matrix provides the best approximation which deviates in the low-temperature limit only slightly from the exact result and almost reaches the ground level for $T \to 0$ K. In all cases in which the high accuracy of the full matrix thawed Gaussian propagator is not required or in which the integration of the equations of motion for the width parameters of a full matrix is too expensive, the frozen Gaussian ansatz with two parameters (2P-FG) seems to be the best choice. It provides the same quality of results as the single-particle thawed Gaussian propagator but is much easier to evaluate since no integrations of parameters of the width matrix are required.

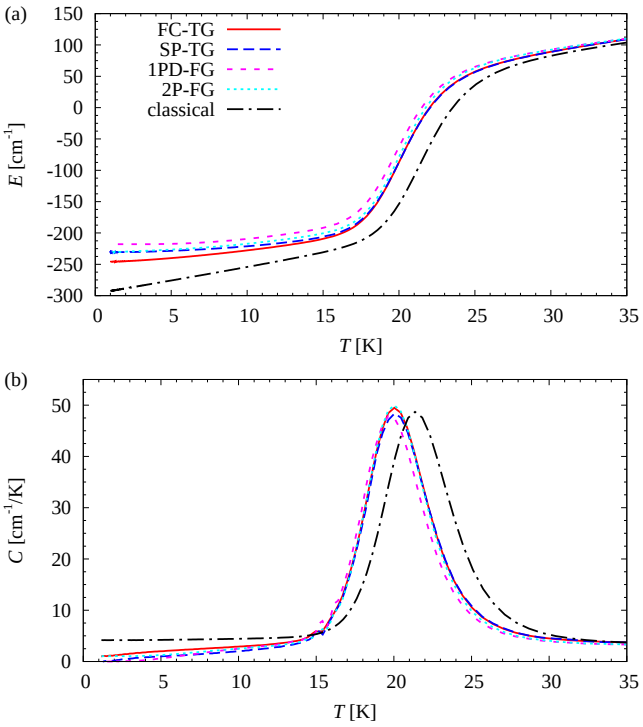

FIG. 3. Mean energy (a) and specific heat (b) of the argon trimer calculated with the Gaussian approximations FC-TG, SP-TG, 1PD-FG, 2P-FG, and classically for $R_c = 32$ Å.

C. Dissociation and the influence of the confining sphere

Before discussing the dissociation process in more detail we have to investigate the influence of the confining sphere on the mean energy and the specific heat. While often a very restrictive value of the confining radius R_c is chosen[1,3,4,7,13], our calculations demonstrate that its value significantly affects the thermodynamic properties of the clusters unless large values, drastically exceeding a few Ångströms, are used. Figure 4 shows the mean energy of the argon trimer for several confinements R_c in a purely classical calculation [Fig. 4(a)] and an evaluation of the quantum partition function with the 2P-FG propagator [Fig. 4(b)], which, as was discussed in Sec. III B, describes the quantum behavior correctly. The values $R_c = 2.6$ Å, 4 Å, and 10 Å have already been used in Ref. 6. The qualitative behavior of these three curves differs strongly. In particular, the mean energy for $R_c = 10$ Å shows a significant increase of the slope for temperatures above 20 K. In Ref. 6 this was regarded as an indication that this radius allows for a total fragmentation of the cluster. However, the mean energy for higher temperatures reveals that this is not fulfilled completely. We included the line for $E = (9/2)kT$ in the figure, which corresponds to three free particles. The mean energy for the restriction $R_c = 10$ Å does not reach that line even at $T = 70$ K. However, for the weaker restrictions $R_c = 15 \ldots 35$ Å one can observe that actually a total

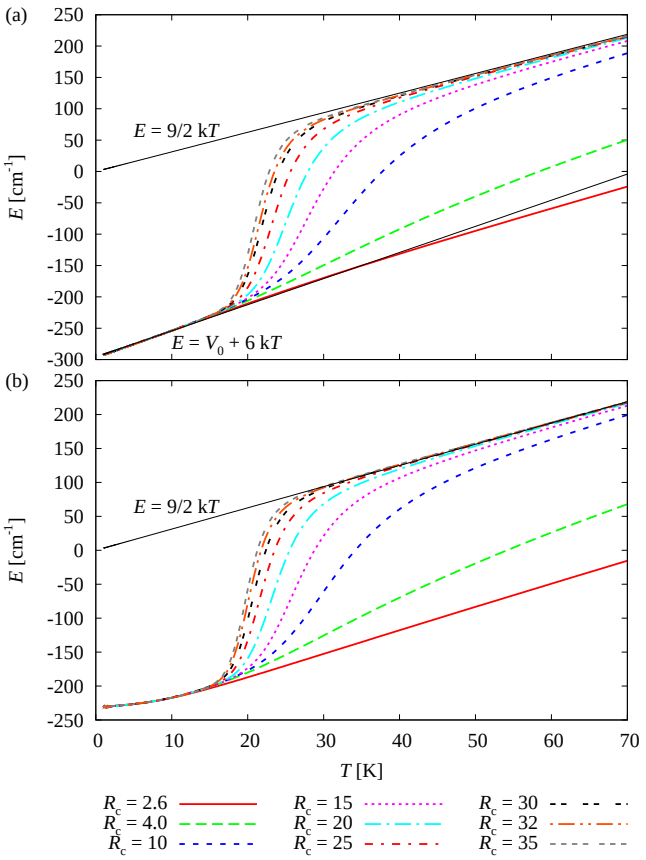

FIG. 4. Comparison of the mean energy of the argon trimer for different confining radii R_c (in Å) in classical (a) and quantum calculations with the 2P-FG partition function (b). We also added the thin black lines $E = 9/2kT$ representing three free particles and $E = V_0 + 6kT$ with the potential minimum $V_0 = -296\,\mathrm{cm}^{-1}$ for the classical low-temperature behavior.

fragmentation takes place and that for $T \gtrapprox 40\,\mathrm{K}$ the energy is identical to that of three free particles. In Fig. 4(a) we also included the line $E = V_0 + 6kT$ with the potential minimum $V_0 = -296\,\mathrm{cm}^{-1}$. This line corresponds to the classical expectation at low temperatures for the internal rotations and oscillations of the trimer plus the energy of the free center of mass.

Even though the behavior at very low ($T \leq 15\,\mathrm{K}$) and high temperatures ($T > 35\,\mathrm{K}$) agrees well for all confinements $R_c > 15\,\text{Å}$ the transition itself obviously depends more critically on the value of R_c. It is clear that a confining radius $R_c = 10\,\text{Å}$ is too restrictive and does not describe the cluster correctly. A significantly larger confining radius $R_c > 30\,\text{Å}$ is required. For the largest confining radii used in Fig. 4 we observe convergence, i.e., a further expansion of the confining sphere does not change the results significantly.

We note that it becomes increasingly difficult to converge the Monte-Carlo integrations for the classical and the 2P-FG partition function for increasing R_c. Similarly, the large error bars in the path-integral Monte Carlo calculation of Ref. 6 indicate that in their computations a radius of $R_c = 10\,\text{Å}$ was already challenging. Nevertheless, the results presented in Fig. 4 demonstrate that the added effort of increasing R_c beyond 30 Å is essential. The necessity for a thorough investigation of the correct boundary conditions is already known from classical investigations of atomic clusters. Etters and Kaelberer[17] demonstrated the negative influence of too restrictive boxes on the classical average energy.

D. Dissociation from classical and quantum perspectives

The cluster at a confinement of $R_c = 32\,\text{Å}$ can be regarded as converged with respect to R_c. The artificial confinement does not have a further noticeable influence on the thermodynamic properties. This allows us to discuss the features observed in the mean energy and the specific heat in more detail. Additionally, the various Gaussian propagators used to obtain the quantum properties agree with each other to a high precision, so that we may consider them as converged in the sense that the choice of Gaussian method has no further influence.

As can be seen in Fig. 3 the qualitative behavior in the quantum and classical cases is almost the same. The cluster is bound at low temperatures, shows a relatively sharp transition, and is completely dissociated for temperatures $T > 33\,\mathrm{K}$. For very low temperatures the classical mean energy exhibits the expected behavior $E \propto 6kT$ [cf. also Fig. 4(a)] for the system (free center of mass, rotations and oscillations of the internal degrees of freedom), whereas the FC-TG mean energy (best approximation, see Sec. III B) converges to a value close to that of the ground level. Further differences between the classical and quantum mechanical results are found in the transition region. It is shifted to slightly lower temperatures in the quantum calculations as compared to the classical. All quantum calculations show a maximum of the specific heat at 20 K, while the classical maximum is at 21.5 K. One reason for this shift is the presence of the zero point energy in the quantum system. As is already obvious in Fig. 4 the classical and quantum results agree very well in the high-temperature limit, since both trend to the case of three free particles. Thus, we conclude that the transition observed in the cluster of three argon atoms is a classical phenomenon. The only difference between classical and quantum mechanics is in the temperature at which the transition occurs. We note that Etters and Kaelberer[17] reported a "liquid-gas transition" identified by the absence of bounded atom configurations in a classical investigation of the system with "free-surface boundary conditions", i.e., without a confining sphere, at $T = 20\,\mathrm{K}$, which is in good agreement with our results.

Our finding of a classical-like complete dissociation of the trimer in one step differs from the conclusions of Pérez de Tudela et al.[6]. While the mean energy in the calculations of Ref. 6 for $R_c = 10\,\text{Å}$ shows a larger and larger slope for increasing temperatures up to $T = 40\,\mathrm{K}$ we ob-

serve already a decrease of the slope for temperatures $T > 30\,\mathrm{K}$. The difference relative to the path-integral Monte Carlo calculations becomes even more pronounced in the specific heat. Pérez de Tudela et al.[6] report that they find an "apparent" maximum which evolves with the radius R_c of the confinement and appears slightly below 40 K for $R_\mathrm{c} = 10\,\text{Å}$. The absence of an unambiguous maximum was seen as an indication for structural changes of the cluster instead of a proper "phase transition". Although the dissociation of the cluster is not fully achieved for such a strong confinement, it is clear from the Gaussian methods used in this article that already for $R_\mathrm{c} = 10\,\text{Å}$ a pronounced peak in the specific heat indicating the dissociation of the system at $T \approx 30\,\mathrm{K}$ is present (cf. Fig. 1). Describing the cluster with a weaker confinement correctly reveals the unambiguous dissociation without intermediate structural modification as discussed above.

The very low temperature found for the dissociation of the cluster may also be important for rare gas clusters in general. As was already discussed[6], even for a confining sphere with $R_\mathrm{c} = 10\,\text{Å}$, the transition temperature of $T \approx 35\,\mathrm{K}$ is lower than temperatures discussed for structural transformations or a "melting" of clusters. Features indicating such changes have, e.g., been found beyond 40 K for argon[25]. If one considers that the dissociation temperature is actually even lower ($T \approx 20\,\mathrm{K}$, c.f. Fig. 3), one necessarily concludes that it is wrong to ignore the influence of the confining sphere on such properties. In larger neon clusters (Ne_{13} and Ne_{38}) features in the mean energy or the specific heat which were related to structural changes, have been reported between 6 K and 8 K[1,3,7]. These temperatures are lower than the dissociation found here, however, one may expect that at least a partial dissociation can set in much earlier in larger clusters since they contain higher energies. In the numerical simulations[1,3,7] the confining radii are chosen such that no atom can leave the cluster during the time evolution. Our results indicate that such a constraint might be too restrictive and lead to incorrect conclusions. A partial or full dissociation can influence structural transformations and may even set in before structural changes of an artificially confined cluster can occur.

IV. CONCLUSIONS AND OUTLOOK

In the present article we investigated the argon trimer by means of semiclassical Gaussian approximations to the Boltzmann operator. We introduced a new matrix structure for a frozen Gaussian variant of the imaginary time propagator which is capable of correctly dealing with the free center of mass motion of a cluster of atoms in Cartesian coordinates. With this matrix structure we were able to show that the frozen Gaussian propagator is, in spite of its simplicity, competitive with numerically more expensive thawed Gaussian variants. In particular, the frozen Gaussian method provides the same quality thermodynamic results as the so-called single-particle thawed Gaussian propagator, which in addition to the time-dependent variables of the frozen Gaussian requires the time evolution for the elements of a block-diagonal width matrix. This is especially true in the low-temperature limit, where quantum effects become important and the form of the semiclassical approximation is supposed to have the largest influence. Our results suggest that the frozen Gaussian ansatz with two parameters (2P-FG) introduced in this article is the method of choice in all cases in which the higher accuracy of the full matrix thawed Gaussian propagator is not required or in which the integration of the equations of motion for the width parameters of a full matrix is too expensive.

The evaluation of the mean energy and the specific heat for the cluster of three argon atoms demonstrated that a previous investigation of the system[6] used too restrictive confinements to describe the dissociation behavior of the system correctly. Above $T = 15\,\mathrm{K}$ the cluster directly dissociates into three free atoms, as is evident from the Gaussian calculations presented in this article. This dissociation is almost purely classical, the influence of quantum mechanics is only found in a convergence to the ground state energy instead of the classical potential minimum for $T \to 0$ and in a slight shift of the three-body dissociation transition to higher classical temperatures ($\Delta T \approx 1.5\,\mathrm{K}$) which we attribute to the zero point energy of quantum mechanics. The clear and pronounced transition found in this article supports the conclusion of Ref. 6 that the dissociation of the atoms from the cluster is important when reconfigurations of the internal structure are considered. Our results strongly indicate that the confinement to very small spheres usually applied in the calculation of the partition function and values deduced from it[1,3,4,13] might be too restrictive to fully understand the low-temperature behavior of the clusters. The dissociation can set in before structural changes or a melting can be observed. To make a clear statement on this question it is necessary to advance the investigations done here to clusters with higher numbers of atoms. In particular, the cases of Ar_6[26], Ar_{13}[26–28], Ne_{13}[3] or Ne_{38}[1] examined recently are of special interest.

On the technical side, it is known that both the frozen and thawed Gaussian propagators used here are, in the framework of a generalized time-dependent perturbation theory[29,30], the lowest order approximations in a series converging to the exact quantum propagator[15,21,24]. Higher orders can help to understand the thermodynamic properties better and to verify the results obtained here with a higher accuracy. Furthermore, the corrections obtained by the evaluation of higher order terms provide objective access to the quality with which the Gaussian approximations reflect the quantum effects in the system studied. They are the topic of current studies.

ACKNOWLEDGMENTS

H.C. is grateful for a fellowship from the Minerva Foundation. This work was supported by a grant of the Israel Science Foundation.

[1] C. Predescu, P. A. Frantsuzov, and V. A. Mandelshtam, J. Chem. Phys. **122**, 154305 (2005).
[2] P. A. Frantsuzov, D. Meluzzi, and V. A. Mandelshtam, Phys. Rev. Lett. **96**, 113401 (2006).
[3] P. A. Frantsuzov and V. A. Mandelshtam, J. Chem. Phys. **121**, 9247 (2004).
[4] C. Predescu, D. Sabo, J. D. Doll, and D. L. Freeman, J. Chem. Phys. **119**, 12119 (2003).
[5] R. P. White, S. M. Cleary, and H. R. Mayne, J. Chem. Phys. **123**, 094505 (2005).
[6] R. Pérez de Tudela, M. Márquez-Mijares, T. González-Lezana, O. Roncero, S. Miret-Artés, G. Delgado-Barrio, and P. Villarreal, J. Chem. Phys. **132**, 244303 (2010).
[7] J. P. Neirotti, D. L. Freeman, and J. D. Doll, J. Chem. Phys. **112**, 3990 (2000).
[8] D. D. Frantz, D. L. Freeman, and J. D. Doll, J. Chem. Phys. **97**, 5713 (1992).
[9] B. J. Berne and D. Thirumalai, Annu. Rev. Phys. Chem. **37**, 401 (1986).
[10] N. Makri, Annu. Rev. Phys. Chem. **50**, 167 (1999).
[11] D. M. Ceperley, AIP Conf. Proc. **690**, 85 (2003).
[12] P. Frantsuzov, A. Neumaier, and V. A. Mandelshtam, Chem. Phys. Lett. **381**, 117 (2003).
[13] P. A. Frantsuzov and V. A. Mandelshtam, J. Chem. Phys. **128**, 094304 (2008).
[14] J. Liu and W. H. Miller, J. Chem. Phys. **125**, 224104 (2006).
[15] D. H. Zhang, J. Shao, and E. Pollak, J. Chem. Phys. **131**, 044116 (2009).
[16] T. González-Lezana, J. Rubayo-Soneira, S. Miret-Artés, F. A. Gianturco, G. Delgado-Barrio, and P. Villarreal, J. Chem. Phys. **110**, 9000 (1999).
[17] R. D. Etters and J. Kaelberer, Phys. Rev. A **11**, 1068 (1975).
[18] D. M. Leitner, R. S. Berry, and R. M. Whitnell, J. Chem. Phys. **91**, 3470 (1989).
[19] D. M. Leitner, J. D. Doll, and R. M. Whitnell, J. Chem. Phys. **94**, 6644 (1991).
[20] P. V. Elyutin, V. I. Baranov, E. D. Belega, and D. N. Trubnikov, J. Chem. Phys. **100**, 3843 (1994).
[21] R. Conte and E. Pollak, Phys. Rev. E **81**, 036704 (2010).
[22] H. Feldmeier and J. Schnack, Rev. Mod. Phys. **72**, 655 (2000).
[23] R. A. Aziz and M. J. Slaman, Mol. Phys. **58**, 679 (1985).
[24] J. Shao and E. Pollak, J. Chem. Phys. **125**, 133502 (2006).
[25] E. Pahl, F. Calvo, L. Koči, and P. Schwerdtfeger, Angew. Chem. Int. Ed. **47**, 8207 (2008).
[26] G. Franke, E. Hilf, and L. Polley, Z. Phys. D **9**, 343 (1988).
[27] P. Borrmann, Comput. Mater. Sci. **2**, 593 (1994).
[28] C. J. Tsai and K. D. Jordan, J. Chem. Phys. **99**, 6957 (1993).
[29] S. Zhang and E. Pollak, Phys. Rev. Lett. **91**, 190201 (2003).
[30] E. Pollak and J. Shao, J. Phys. Chem. A **107**, 7112 (2003).